sciendo

Bio-Algorithms and Med-Systems 2022; 18(1):171-179

Research article

Martyna Durak-Kozica*, Andrzej Wróbel, Mark Platt and Ewa Ł. Stępień

Comparison of qNANO results from the isolation of extracellular microvesicles with the theoretical model

https://doi.org/10.2478/bioal-2022-0088
Received December 12, 2022; accepted December 13, 2022; published online December 19, 2022.

Abstract: Objectives: Extracellular vesicles (EVs) are heterogeneous membrane vesicles in diameter of 30-5000 nm, that transport proteins, non-coding RNAs (miRNAs), lipids and metabolites. Major populations include exosomes, ectosomes and apoptotic bodies. The purpose of this study was to compare the distribution of EVs obtained under different conditions of differential centrifugation, including ultracentrifugation, with the results developed based on a theoretical model. Methods: Immortalized endothelial cell line that expresses h-TERT (human telomerase) was used to release of EVs: microvascular TIME. EVs were isolated from the culture medium at different centrifugation parameters. The size distribution of the EVs was measured using TRPS technology on a qNano instrument. Surface markers were evaluated using flow cytometry. The isolated EV subpopulations were compared with the theoretical model developed by Livshits. Results: EVs isolated from endothelial cells show strong aggregating properties, which was confirmed by TEM, TRPS imaging and flow cytometry. Conclusions: Obtaining pure EV subpopulations is difficult because of the small differences in the diameter of ectosomes and exosomes, and the strong aggregating properties of EVs.

Keywords: ectosomes, exosomes, endothelial cells, differential centrifugation.

***Corresponding author: M. Durak-Kozica**, Marian Smoluchowski Institute of Physics, Department of Medical Physics, Marian Smoluchowski Institute of Physics Faculty of Physics, Astronomy and Applied Computer Science, Jagiellonian University, Krakow, Poland; Centre for Theranostics, Jagiellonian University, Kraków, Poland, Phone: +48 12 664 47 62, E-mail: durakmartyna@gmail.com

A. Wróbel, Marian Smoluchowski Institute of Physics, Department of Medical Physics, Marian Smoluchowski Institute of Physics Faculty of Physics, Astronomy and Applied Computer Science, Jagiellonian University, Krakow, Poland; Centre for Theranostics, Jagiellonian University, Kraków, Poland

M. Platt, Department of Chemistry, Loughborough University, Loughborough, United Kingdom

E. Ł. Stępień, Marian Smoluchowski Institute of Physics, Department of Medical Physics, Marian Smoluchowski Institute of Physics Faculty of Physics, Astronomy and Applied Computer Science, Jagiellonian University, Krakow, Poland; Centre for Theranostics, Jagiellonian University, Kraków, Poland, Phone: +48 12 664 47 62, E-mail: e.stepien@uj.edu.pl; Total-Body Jagiellonian-PET Laboratory, Jagiellonian University, Kraków, Poland

Introduction

Extracellular vesicles (EVs) are defined as cellular structures surrounded by a protein-lipid membrane secreted by almost all cell types [1-5]. They play an important role in physiological and pathological processes, mediating extracellular transport and transferring various types of intracellular, secretory and membrane proteins, as well as nucleic acids such as small molecule RNA, mRNA, and others [6-9]. In recent years, the role of EVs in regenerative medicine has been extensively studied. EVs from different cell types create therapeutic potential in an increasing number of different, as a biomarker, therapeutic agent or drug carrier [10-12]. The average size of EVs is estimated between 30 and 500 nm and covers the range of smaller exosomes (30-100 nm in diameter) and bigger ectosomes (over 100 nm in diameter) [12].

Liquid biological samples are usually heterogeneous mixtures of particles that differ in size and density, as well as in sedimentation rate, such physical properties can be utilized for developing modern isolation and separation techniques [13].

The classic protocol for acquiring EVs from a conditioned medium uses differential centrifugation [14]. It is a physical technique that has wide application

in biological research for the isolation and purification of cells, viruses, intracellular organelles, etc. from suspensions, such as cell lysates or cell culture supernatant. As a result of centrifugation, particles with a higher density than the solvent are sedimented, and with a density lower than this are floated [15]. Liquid biological samples are usually heterogeneous mixtures of particles that differ in size and density, and also in sedimentation rate, such physical properties can be utilized for developing modern isolation and separation techniques [16].

In the research carried out for this work, a model based on the differential centrifugation principles was used to calculate parameters for EVs isolation and set experimental conditions. The model proposed by Mikhail A. Livshits takes into account the following points used in the equations and used for further considerations: geometric parameters of the rotor, angular velocity (ω), centrifugation time (t), and solution viscosity (η) [15].

The theoretical model introduced by Livshits allows us to evaluate the proportion of deposited EVs with specific sizes (30-1,000 nm) and densities (1.08-1.15 g/cm^3). Based on the equations and geometric relationships for FA-type rotors, the yield (efficiency) parameter of the centrifugation process (pelleted fraction - PF_d) was developed, i.e., the fraction of particles with a diameter d, that after time t, will cover the distance L_{sed}:

$$PF_d = \frac{2}{\pi}\left(\arcsin\frac{vt}{L_{sed}} + \frac{vt}{L_{sed}}\sqrt{1-\left(\frac{vt}{L_{sed}}\right)^2}\right) \quad (1)$$

Bearing in mind the limitations of preparing homogeneous isolations of EV subpopulations, the main purpose of this work was to determine the differential centrifugation parameters to isolate two pure EV subpopulations, based on this model.

Materials and methods

Cell culture

A human immortalized microvascular endothelial cell line (TIME) that expresses human telomerase (h-TERT) was used [16]. TIME cells were grown in Vascular Cell Basal Medium (ATCC; PCS-100-030) supplemented with penicillin (100 U/ml), streptomycin (100 U/ml), blasticidin (12.5 µg/ml), and the microvascular supplement kit Endothelial Cell Growth Kit-VEGF (ATCC PCS-110-041). Cells were grown in 75 cm^2 tissue culture dishes (Nest Scientific Biotechnology, China) at 37◦C in an incubator with a humidified mixture of 5% CO_2 and 95% air. For EVs isolation, cells were incubated for 48h in a medium with exosome-free FBS (Gibco, A2720801).

Experimental results vs theoretical model

To compare the experimental results with the theoretical model, EV isolation was performed at different centrifugation speeds (Fig. 1). The medium was initially centrifuged for 30 minutes at 2,000 ×g to remove cells and apoptotic bodies. The medium thus obtained contained a population of ectosomes and exosomes. Ectosomes were isolated from the culture medium by centrifugation at 3,000, 5,000, 7,000, 10,000, 12,000 or 18,000 xg for 30 min at 4°C. The harvested supernatant was then centrifuged for 90 min at 150,000 xg at 4°C. The obtained EV pellets were suspended in 100 µl of filtrated PBS.

Two different centrifuges equipped with fixed-angle rotors were used in the tests: S140-AT and FA-45-24-11. The basic rotor parameters are shown in Tab.1.

In the presented model, calculations were made based on Equation 1. It was assumed that the values of EV density (p) and the medium viscosity (η) are with the ranges as in Tab.1 and have a homogeneous distribution.

The isolated EV populations were diluted 2-fold and filtered through a filter with a pore diameter of 400 nm. To determine the microvesicle diameter distribution, TRPS technologies were used on a qNano apparatus (Izon Science Ltd.) equipped with NP100 pore (Izon Science Ltd.).

The yield (efficiency) of the model for pelleted ectosomes PF_{Ecto} was determined directly from the relationship (Equation1), using the parameters defined in Tab1. For exosomes, the efficiency is described by the Equation 2:

$$PF = PF_{Exo} - (1 - PF_{Ecto}) \quad (2)$$

Fortran 90 program (Simply Fortran 2.41, Approximatrix.) was used for numerical estimation of centrifugation efficiency based on Equation 1 and model density distributions for particular values of the relative centrifugal force [18]. Density distributions were calculated based on the results of qNano measurements for pre-centrifuged EV suspension. The program generated the results for randomly selected values of EV density and viscosity of the medium from the given ranges (Tab.1) (Figure 3C and 3D). A random number

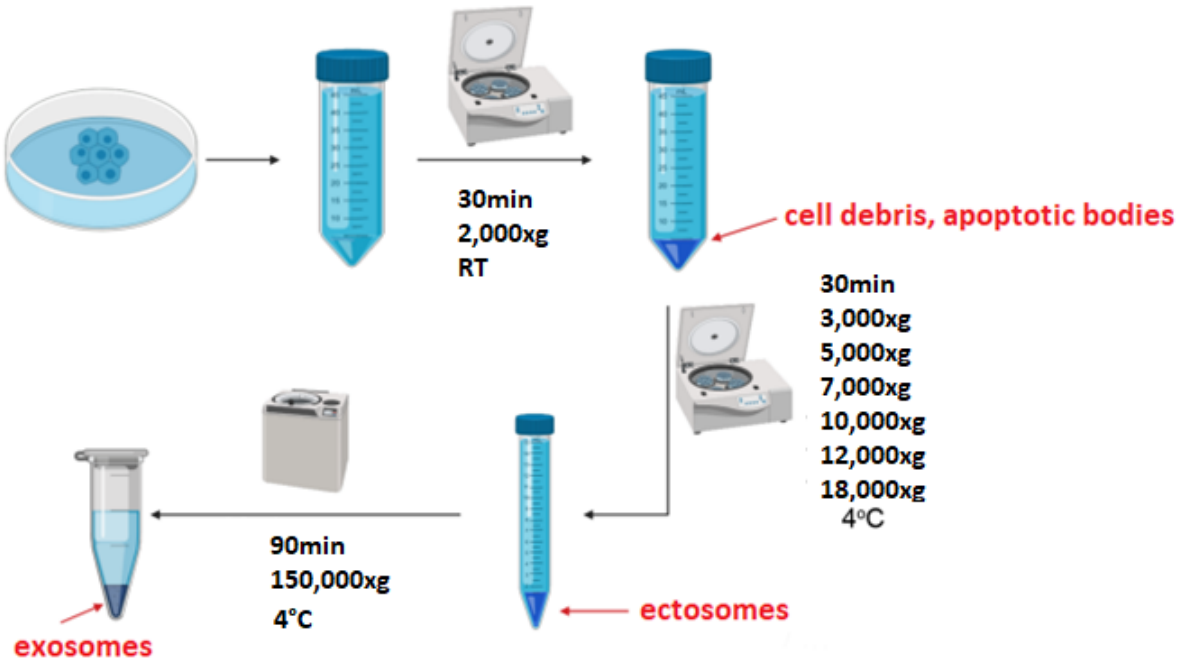

Figure 1: Scheme of EV isolation and separation steps using differential centrifugation for comparison with the theoretical model.

	S140-AT	FA-45-24-11
R_{min}[cm]	3.26	7.58
R_{max}[cm]	4.79	11.07
θ [°]	35	45
Tube diameter [cm]	0.75	0.85
ρ [g/cm^3]	1.1 ÷ 1.3[17]	1.1 ÷ 1.3[17]
ρ_{solv} [g/cm^3]	1.0#	1.0#
η [cP]#	1÷1.5	1÷1.5
Relative Centrifugal Force RCF	150,000g	2,000-18,000g
Time [min]	90	30

Table 1: Parameters of rotors, centrifugation, and physical parameters of the medium and EVs #medium viscosity value rounded to 1cP based on measurements viscosity.

generator with a homogeneous distribution was used in the calculations. The resulting text files contain the values of: centrifugation efficiency, density distributions $d_{cut\ off}$. and randomized densities and viscosities used in the calculations [18]. Based on these files. The results were presented graphically using the Grapher 11 program.

EV isolation

Subconfluent TIME cell cultures were incubated for 48 h in a culture medium supplemented with 2% exosome-free FBS. The culture medium was then collected into tubes and centrifuged for 30 min at 2,000 x g to remove floating cells and apoptotic bodies. The pre-centrifuged medium was centrifuged for 30 min at 18,000 × g to pellet the

ectosome. The collected supernatant was centrifuged for 90 min at 150,000 x g and 4°C to obtain the exosome pellet. The resulting ectosome and exosome pellets were suspended in 100 µl of PBS.

TRPS method to characterize EV size and concentration and Zeta-potential

The size distribution and concentration of EVs were measured by TRPS technology using the qNano system (Izon Science Ltd.. Oxford. UK). The instrument was calibrated using CPC100 and CPC200 calibration particles (Izon Science) according to the manufacturer's instructions. Exosomes were measured using NP100 nanopores (analysis range 50-330 nm; Izon Science) at a pressure of 5 mbar. Ectosomes were measured using NP200 nanopores (analysis range 85-500 nm; Izon Science) with at 1 mbar pressure. Voltage and stretch were adjusted to obtain a stable current between 100-120 nA. The samples were analyzed for 3 minutes or until the measurement was performed on 500 objects. Data processing and analysis were prepared using the Izon Control Suite v2.2 software (Izon Science).

To measure the Zeta-potential for ectosomes (isolated at 18.000xg) and exosomes, nanopores were calibrated at three different voltages (V1, V2, V3) and two different pressures (P1, P2) (Tab.2). The microvesicles samples were measured at a voltage of V2 and pressure P2.

Calibration	Pressure[mbar]	Voltage[mV]
V1P2	0.1	0.94
V1P1	1.1	0.94
V2P1	1.1	0.76
V3P1	1.1	0.60

Table 2: The value of pressure and voltage at the performed nanopore calibration.

Visualization of EVs using a transmission electron microscope (TEM)

The exosome and ectosome pellets were fixed with 2.5% glutaraldehyde (Sigma Aldrich, cat. No. G5882) in 0.1 M cacodyl buffer (Sigma Aldrich, cat. No. CO250) and then fixed for 1 hour in 1% osmium oxide. The samples were then dehydrated by passing through a graduated series of ethanol and embedded in PolyBed 812 epoxy resin at 68°C (Polyscience, Inc., Cat # 08791-500). The ultra-thin (65-70 nm) sections were placed on 300 mesh copper grids covered with formvar foil. The sections were contrasted with uranyl acetate and lead citrate. The observation was performed with an electron microscope (JEOL JEM2100HT, Jeol Ltd, Tokyo, Japan) at an accelerating voltage of 80 kV. The microvesicle diameters were determined manually in the Fiji program version 2.9.0.

Flow cytometry to determine EV surface markers

Surface markers on TIME EVs were detected with Micro Apogee A50 flow cytometer (ApogeeFlow Systems, Hemel Hempstead, UK) after staining with anti-CD63 (BioLegend, ABIN1998604), anti-CD151 (BioLegend, ABIN2478583) annexin V (Invitrogen, Aforem122) and annexin-binding buffer antibodies (Invitrogen, V13246). The murine IgG1 FITC / IgG1 PE / IgG1 PE-Cy5 IsotypeCtrl Cocktail (BioLegend, 319201) antibody was used as an isotope control. All antibodies were centrifuged for 5 minutes at 18,890 x g to remove dye aggregates. Ectosomes and exosomes suspended in PBS (Sigma) were incubated with selected antibodies for 30 minutes in the dark. Positive event percentage (ROI% event) was calculated with the Apogee Histogram software (ApogeeFlow Systems).

Results

Theoretical model development and its verification

The results of the yields calculations for a given value of EV density (ectosomes and exosomes) 1.15 g/cm^3 and the solvent viscosity of 1.03 cP for ectosomes and exosomes are presented in Fig. 2A. The highest efficiency of ectosome deposition during centrifugation was observed at 18,000 x g, while also observing the cut-off point at the smallest exosome size.

Density and viscosity values were randomly selected from the ranges in Table 1, assuming that both the density and viscosity values were derived from a homogeneous distribution. In Fig. 2C, we can see that centrifugation at 18,000 x g is the limit above which the ectosome sedimentation efficiency does not depend on the physical properties of the EV (density) and on the solvent (viscosity). Centrifugation above 18,000 x g would greatly reduce the concentration of the isolated

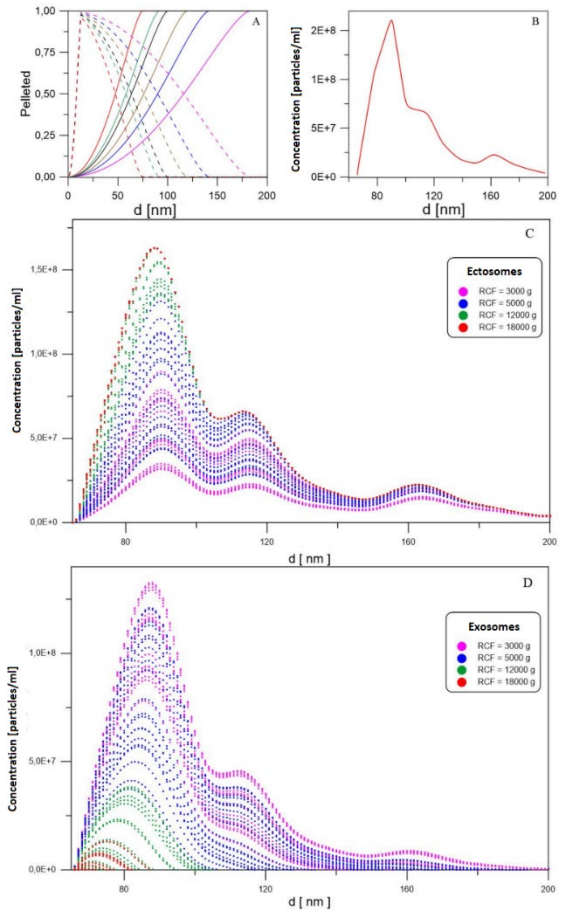

Figure 2: A) Centrifugation yields calculated from the theoretical model for ectosomes (solid line) and exosomes (line dotted line). PF was calculated from equation 1 and 2 based on data contained in Tab.1, B) initial concentration of EV distribution determined based on the measurements of qNano, C and D predicted distribution / concentration of exosomes and ectosomes. Areas for individual values of relative centrifugal force are between the highest and lowest of the selected measurement points.

exosomes, however, we see that with these centrifugation parameters we should get the purest ectosomes population by cutting off the EV size above 100nm.

Figures 3A and 3B show a comparison of the theoretical predictions with the measurements of EV diameters using the TRPS method. Based on data contained in the work, measurement error in determining the of EV diameter using the qNano method, is ± 10 nm [19]. For theoretical calculations, the figures show the range of concentration values calculated in the draws. Figure 3A shows that centrifugation at 12,000 x g and 18,000 x g gives the ectosome population closest to the theoretical model. In contrast, Fig 3B shows that the population of exosomes isolated from the supernatants after centrifugation at lower g values (5,000 – 10,000 x g)

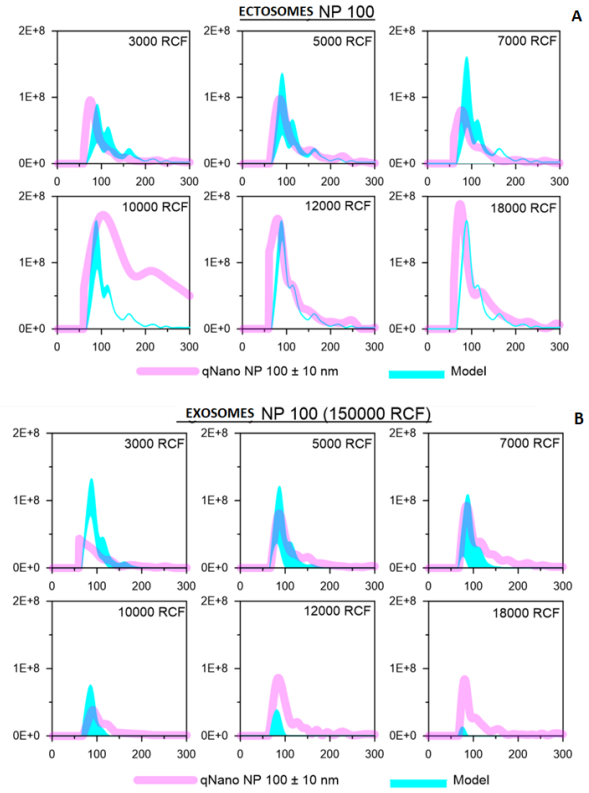

Figure 3: Comparison of theoretical results with qNano (TRPS). The measurement error shown in the figure is ±10nm. Measurements for A) ectosomes, B) exosomes.

is closer to the results of the theoretical model. Based on these results, we chose to centrifuge the ectosomes for the remainder of the research at 18,000 x g.

Zeta potential measurements

The measured Zeta – potential for ectosomes was −9.3 ± 0.7 mV and for exosomes −11.35 ± 1.9 mV (Fig.4.). The yellow line indicates the maximum value of the ectosomes/exosomes as the limit in the theoretical model. Taking into account the above assumption, the average Zeta-potential value changed −9.53 ± 0.52 mV for ectosomes and −17.05 ± 0.79 mV for exosomes.

Visualization of EVs by TEM

Transmission electron microscopy (TEM) was used to visualize isolated populations of ectosomes and exosomes. Analysis of the EV images showed the size of both ectosomes and exosomes in the range of 10-400 nm. The obtained images showed the heterogeneity of the resulting EV populations. A double membrane characteristic of EVs was observed (Fig.5A). Fitting the multi-peak Lognormal function showed the presence of

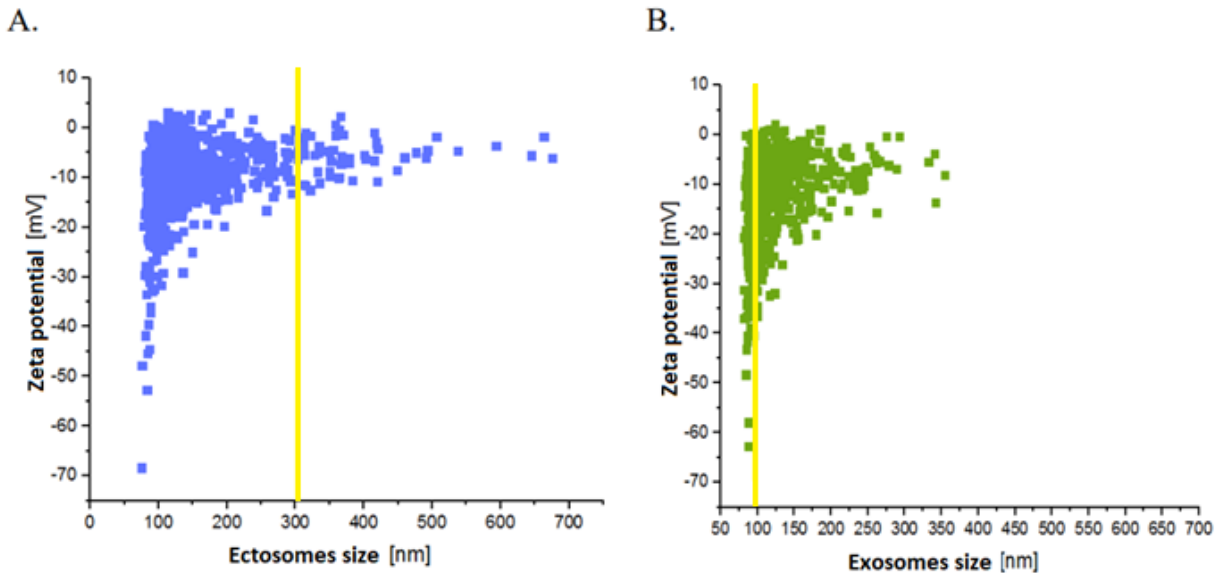

Figure 4: Dependence of Zeta-potential of EVs on their diameter. A. Ectosomes, B. Exosomes.

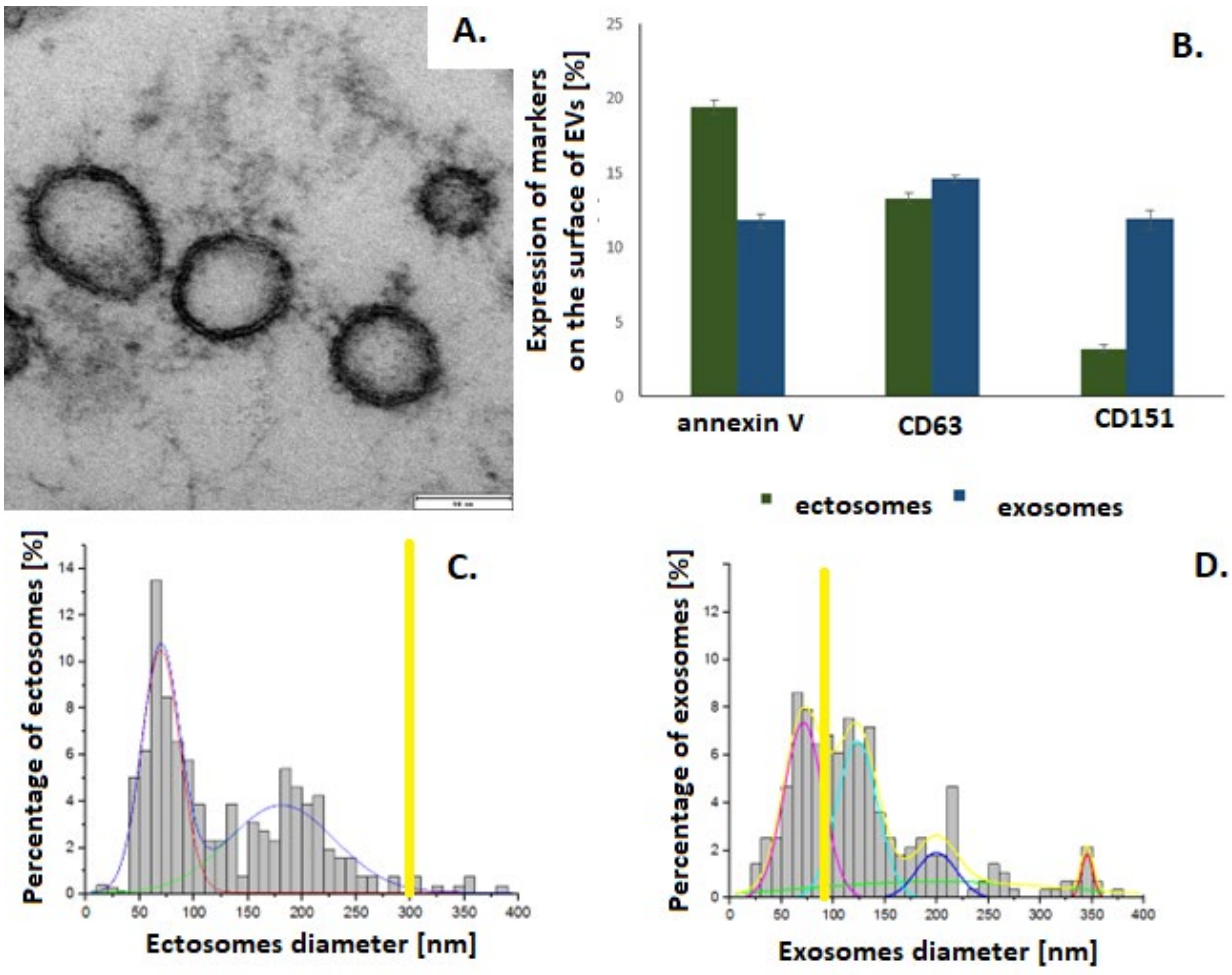

Figure 5: A) EVs visualized in a TEM microscope, a lipid bilayer can be observed. B) Analysis of annexin V. CD151, and CD63 expression on the EV surface. C) Size distribution of ectosomes; and D) exosomes with a fit of the multi-peak Lognormal function. The yellow line shows the limit value calculated from the theoretical model.

two major ectosome populations of 69.35 and 181.14 nm and the presence of four major exosome populations: 71.06; 122.85; 199.66 and 345.22 nm in diameter (Fig. 5C and 5D).

Analysis of surface markers using Apogee flow cytometry

Annexin V is a commonly used as an ectosome marker. CD63 and CD151 are exosomal markers. The measurements confirmed the TEM observations, indicating cross-contamination of the population.

Results

The applied centrifugation parameters from 3000 to 18000 x g for ectosomes showed distributions of obtained EVs similar to the theoretical data calculated based on the Mikhail A. Livshits model [15]. On the other hand, the greatest discrepancies for the exosome population were obtained for the supernatant after centrifugation at 18,000 x g. Our results showed cross-contamination of two EV sub-populations. These observations were confirmed by TEM and flow cytometry.

The most common procedure for the isolation of exosomes involves ultracentrifugation at 100,000-200,000 x g [14]. while for ectosomes centrifugation at 10,000-20,000xg [20]. Our results indicated cross-contamination of the EV subpopulation, and exosome sedimentation at centrifugation speed in the range of 3,000 x g – 18,000 x g, which has been observed by other authors as the sedimentation of exosomes at 33,000xg [21].

In the presented work, we performed measurements using qNano (TRPS), which is an increasingly used method for analyzing the size, concentration and Zeta-potential of EV, as well as nanoparticles. liposomes. etc. [22,23]. The advantage of this method is the small volume of the analyzed sample, and the possibility of precise indication of particles of different sizes. However, the practical limitation to measuring biological samples with TRPS is pore plugging. Accumulating bulky proteins (e.g. von Willebrand factor. fibrinogen) or the presence of particles with a diameter larger than the pores (e.g. aggregates microvesicles) may contribute to pore clogging [24].

To study the stability of the isolated EV subpopulations, the Zeta-potential was measured. The obtained values for ectosomes (-9.3 ± 0.7 mV) and exosomes (-11.35 ± 1.9 mV) indicated EV aggregation properties. The value of -10 mV is generally recognized as a minimum threshold value for sample stability in dispersion [25,26]. The obtained results are similar to those obtained by Duc Bach Nguyen et al., who demonstrated the Zeta-potential of EVs isolated from reds blood cells within -10 mV [27].

Based on the data in Table 1 (i.e. size range of both microvesicle populations) and Equitation 1, the sedimentation coefficient was calculated for both EV fractions. The S_{exo} value ranges from 72.8 to 1160 S and the S_{ecto} value from 809 to 81000 S. The overlap of the range of sedimentation coefficient values for both EV populations causes cross-contamination of samples, what we demonstrated in our work. The optimization process is less effective when there are small variations in sedimentation coefficients between different particle fractions ($S_{exo} \approx S_{ecto}$).

EV density values are close to protein density, showed that proteins (e.g. plasma albumin or fibrinogen in plasma) are sediment with EVs during centrifugation. Using Equations 1 and 2, we calculated the yield sedimentation of the folded and unfolded forms of the proteins mentioned above. Exists are unlikely to sediment albumin (66.5 kDa) in any fraction of microvesicles. Also, the efficiency of fibrinogen sedimentation is low because in solutions it is present in solution in the coiled form [18,28] (supplementary file).

TEM analysis of exosomes and ectosomes showed a regular oval shape of EVs surrounded by a lipid bilayer. A similar shape of the EVs was also observed by others researchers working on an endothelial cell line and a human leukemic line [29]. Microscopic analysis showed cross-contamination of the EVs samples. It was also confirmed by marker expression analysis i.e. CD63 and CD151 (exosome markers) and annexin V (ectosome marker). Similar observations about ARF6 (exosome marker) expression were made on EVs isolated from breast cancer lines [30].

Conclusion

Development of an EV isolation protocol based on the theoretical model is possible and useful to obtain homogeneous subpopulations of ectosomes and exosomes. Validation under experimental conditions is difficult due to the small size difference in diameter size. Additionally, strong aggregation properties of

endothelial-derived EVs were proven as low Zeta-potential of EVs isolated from endothelial cells.

Acknowledgements

This publication contains part of Martyna Durak-Kozica's Ph.D.Ph.D. dissertation. This work was funded by National Science Center, grant PRELUDIUM 8 number UMO-2014/15/N/NZ5/01606.

The authors want to express their gratitude to Dr. Eng. Olga Woźnicka from the Microscopy Laboratory of the Institute of Zoology and Biomedical Research, the Jagiellonian University, for specimen preparation and TEM imaging.

Author contributions

All authors have accepted responsibility for the entire content of this manuscript and approved its submission.

Competing interests

The authors state no conflict of interest.

References

[1] Stępień EŁ, Rząca C, Moskal P, Radiovesicolomics-new approach in medical imaging. Front Physiol 2022;13:996985. doi: 10.3389/fphys.2022.996985.

[2] Marzec ME, Rząca C, Moskal P, Stępień EŁ, Study of the influence of hyperglycemia on the abundance of amino acids, fatty acids, and selected lipids in extracellular vesicles using TOF-SIMS. Biochem Biophys Res Commun 2022;622:30-36. doi: 10.1016/j.bbrc.2022.07.020.

[3] Tokarz A, Konkolewska M, Kuśnierz-Cabala B, Maziarz B, Hanarz P, Żurakowski A, Szuścik I, Stępień EŁ, Retinopathy severity correlates with RANTES concentrations and CCR 5-positive microvesicles in diabetes. Folia Med Cracov 2019;59(3):95-112. doi: 10.24425/fmc.2019.131139.

[4] Stępień EŁ, Kamińska A, Surman M, Karbowska D, Wróbel A, Przybyło M. Fourier- Transform InfraRed (FT-IR) spectroscopy to show alterations in molecular composition of EV subpopulations from melanoma cell lines in different malignancy. Biochem Biophys Rep 2021;25:100888. doi:10.1016/j.bbrep.2020.100888.

[5] Kim DK, Lee J, Kim SR, Choi DS, Yoon YJ, Kim JH, Go G, et al. EVpedia: a community web portal for extracellular vesicles research. Bioinformatics 2015;31(6):933-9. doi: 10.1093/bioinformatics/btu741.

[6] Stępień EŁ, Durak-Kozica M, Kamińska A, Targosz-Korecka M, Libera M, Tylko G, Opalińska A, Kapusta M, Solnica B, Georgescu A, Costa MC, Czyżewska-Buczyńska A, Witkiewicz W, Małecki MT, Enguita FJ. Circulating ectosomes: Determination of angiogenic microRNAs in type 2 diabetes. Theranostics 2018;8(14):3874-3890. doi: 10.7150/thno.23334.

[7] Kamińska A, Roman M, Wróbel A, Gala-Błądzińska A, Małecki MT, Paluszkiewicz C, Stępień EŁ. Raman spectroscopy of urinary extracellular vesicles to stratify patients with chronic kidney disease in type 2 diabetes. Nanomedicine: NBM 2022;39:102468. doi: 10.1016/j.nano.2021.102468.

[8] Drożdż A, Kołodziej T, Wróbel S, Misztal K, Targosz-Korecka M, Drab M, Jach R, Rząca C, Surman M, Przybyło M, Rajfur Z, Stępień EŁ. Large extracellular vesicles do not mitigate the harmful effect of hyperglycemia on endothelial cell mobility. Eur J Cell Biol 2022;101(4):151266. doi: 10.1016/j.ejcb.2022.151266.

[9] Lima TSM, Souza W, Geaquinto LRO, Sanches PL, Stępień EL, Meneses J, et al.. Nanomaterial exposure, extracellular vesicle biogenesis and adverse cellular outcomes: A Scoping Review. Nanomaterials (Basel) 2022;12(7):1231. doi: 10.3390/nano12071231.

[10] Gąsecka A, van der Pol E, Nieuwland R, Stępień E. Extracellular vesicles in post-infarct ventricular remodelling. Kardiol Pol 2018;76(1):69-76. doi: 10.5603/KP.a2017.0178.

[11] Roman M, Kamińska A, Drożdż A, Platt M, Kuźniewski M, Małecki MT, Kwiatek WM, Paluszkiewicz C, Stępień EŁ. Raman spectral signatures of urinary extracellular vesicles from diabetic patients and hyperglycemic endothelial cells as potential biomarkers in diabetes. Nanomedicine: NBM 2019;17:137-149. doi: 10.1016/j.nano.2019.01.011

[12] Ewa Ł. Stępień , Carina Rząca , Paweł Moskal. Novel biomarker and drug delivery systems for theranostics: extracellular vesicles 10.1515/bams-2021-0183.

[13] Liangsupree T, Multia E, Riekkola ML. Modern isolation and separation techniques for extracellular vesicles. J Chromatogr A. 2021;1636:461773. doi:10.1016/j.chroma.2020.461773.

[14] Théry C, Amigorena S, Raposo G, Clayton A. Isolation and characterization of exosomes from cell culture supernatants and biological fluids. Curr Protoc Cell Biol 2006; Chapter 3. doi:10.1002/0471143030.cb0322s30.

[15] Livshits MA, Khomyakova E, Evtushenko EG, Lazarev VN, Kulemin NA, Semina SE, et al Isolation of exosomes by differential centrifugation: Theoretical analysis of a commonly used protocol. Sci Rep 2015;5:17319.

[16] Durak-Kozica M, Baster Z, Kubat K, Stępień E. 3D visualization of extracellular vesicle uptake by endothelial cells. Cell Mol Biol Lett. 2018;23:57doi:10.1186/s11658-018-0123-z.

[17] Zhang, Y., Y. Liu, H. Liu, W. H. Tang,. Exosomes: biogenesis, biologic function, and clinical potential. Cell & bioscience 2019; 9:19.

[18] Stępień E, Durak-Kozica M, Wróbel A, Platt M. (2022). Tunable Resistive Pulse Sensing results from the isolation of extracellular microvesicles in comparison with the theoretical model. Repozytorium Uniwersytetu Jagiellońskiego. https://doi.org/10.26106/vngy-9551

[19] IZON SCIENCE LIMITED. Tunable Resistive Pulse Sensing: Essential information about nanoparticles is revealed quickly and accurately. www.izon.com.

[20] Witwer KW, Buzas EI, Bemis LT, Bora ., Lasser C, Lotvall J, Standardization of sample collection, isolation and analysis methods in extracellular vesicle research. J Extracell Vesicles 2013; 2:1-25.

[21] Jeppesen DK, Hvam ML, Primdahl-Bengtson B, Boysen AT, Whitehead B, Dyrskjøt L. et al. Comparative analysis of discrete exosome fractions obtained by differentia centrifugation. J Extracell Vesicles 2014: 3:25011.

[22] Greenberg JW, Kim H, Moustafa AA, Datta A, Barata PC, Boulares AH et al. Repurposing ketoconazole as an exosome directed adjunct to sunitinib in treating renal cell carcinoma. Sci Rep 2021;11(1):1-2.

[23] Maas S.L., De Vrij J., Broekman M.L., Quantification and Size-profiling of Extracellular Vesicles Using Tunable Resistive Pulse Sensing. J Vis Exp, 2014; 92:51623.

[24] van der Pol E, Coumans F, Varga Z, Krumrey M, Nieuwland R, Innovation in the detection of microparticles and exosomes. J Thromb Haem 2013; 1:36-45.

[25] Soares Martins T, Catita J, Martins Rosa I, AB da Cruz E, Silva ., Henriques AG, Exosome isolation from distinct biofluids using precipitation and column-based approaches. PLOS ONE 2018;13: 0198820.

[26] Midekessa G, Godakumara K, Ord J, Viil J, Lättekivi F, Dissanayake K et al. Zeta potential of extracellular vesicles: toward understanding the attributes that determine colloidal stability. Acs Omega. 2020 Jun 30;5(27):16701-10.

[27] Nguyena D.B., Ly T.B., Wesseling M.C., Hittinger M., Torge A., Devitt A., Perrie Y., Bernhardt I., Characterization of microvesicles released from human red blood cells, Cell Phys Biochem 2016;38:1085-1099

[28] Zhmurov A, Brown AEX, Litvinov RI, Dima RI, Weisel JW, Barsegov V, Mechanism of fibrin(ogen) forced unfolding. Structure 2011;19:1615–1624.

[29] Gao J, Wang S, Wang Z, Yield H. Scalable and remotely drug-loaded neutrophilderived extracellular vesicles (EVs) for anti-inflammation therapy, Biomaterials. 2017;135:62–73.

[30] Durrieu ., Bharadwaj A, Waisman DM, Analysis of the thrombotic and fibrinolytic activities of tumor cell–derived extracellular vesicles. Blood Adv 2018; 2:1054-1065 139

[31] Patel GK. Comparative analysis of exosome isolation methods using culture supernatant for optimum yield, purity and downstream applications. Scie Rep 2019;9:5335